224 (2023) 211599

Contents lists available at ScienceDirect

Geoenergy Science and Engineering

journal homepage: www.sciencedirect.com/journal/geoenergy-science-and-engineering

Experimental investigation of the development of surfactant stabilized oil-water pipe flow downstream of a choke valve

Heiner Schümann *, Galina Simonsen, Christian Brekken

Department of Process Technology, SINTEF AS, Strindvegen 4, NO-7034, Trondheim, Norway

ARTICLE INFO

Keywords:
Oil-water dispersions
Droplet size distributions (DSD)
Flow development
In-situ separation
Span 83

ABSTRACT

In wells and multiphase flowlines the presence of valves, pumps and other complex geometries will considerable contribute to dispersion of the phases. In combination with the droplet stabilizing effect of natural surfactants contained in the crude oil and other production chemicals, this may lead to a considerable development length of the flow. Such effects should be understood and considered by future simulation tools. In the presented work, the described scenario was experimentally tested under controlled conditions. The development of dispersed oil-water flow downstream of a valve was monitored. Surfactant was added to the mineral oil to obtain a suitable droplet stability. The near horizontal test section was 220 m long and had an inner diameter of 109 mm. The vertical phase fraction distributions were measured at six locations along the pipe with traversing gamma densitometers. The test section was further instrumented with nine pressure transducers, four optical sections, and three droplet sampling points to monitor flow development. The flow development showed a characteristic behavior of a rather sudden separation after a certain length with stable dispersed flow conditions. The degree of inlet mixing and thus initial droplet size governed by the pressure drop over the mixing valve was found to be crucial for the development length. Flow rate and initial water fraction were of minor importance. The separation behavior was coalescence controlled as it would be expected for a surfactant stabilized system. Still, even if static separation bench tests resulted in very long separation time scales, the in-flow separation happened much faster. This indicates the importance of dynamic flow conditions and associated effects such as shear and a certain mixing to be preferential for the separation. The measured pressure drop of the dispersed flow was more than 20% higher than separated flow with otherwise the same conditions. As the flow separates, the pressure drop decreases and, as expected, finally approaches the value for separated flow. The work presents a detailed data set as basis for model development.

1. Introduction

Flow of two immiscible fluids occurs in a variety of engineering applications. The main motivation for the presented research is the simultaneous occurrence of crude oil and water in wells and transport lines of oil production systems. Such transport systems, often many kilometres in length, must be operated in an efficient and predictable way. The flow resistance must be minimized to ensure smooth and energy efficient operation. Furthermore, the so-called flow pattern in the pipe, describing the spatial distribution of the fluid phases, should be known. In particular, the occurrence of free water in the pipe is of major interest in corrosion and hydrate formation risk assessment.

Typically, in mature fields water is produced along with the oil and can even be the dominating phase at the end of a field's lifetime. The occurrence of oil-water dispersions, or emulsions in the case of a stable dispersion, plays a critical role in this context. Flow properties of dispersions can differ strongly from those of the pure phases. The effective viscosity of a dispersion can be many times higher than that of the continuous phase. As documented by Pal (Pal and Rhodes, 1989; Pal, 1993, 1996), this effective dispersion viscosity is mainly a function of the dispersed phase fraction and continuous phase viscosity. However, other factors such as the dispersed phase viscosity, droplet size or the presence of stabilizing components or surfactants may also play a role. Oil and water will, in many cases, already be dispersed when entering the well. Pumps and valves in the production system will contribute to further breakage of the droplets. Regarding the multiphase flow itself, two effects must be considered. On the one hand, high velocities or steeply inclined pipe orientation will promote dispersed flow. On the

* Corresponding author.
E-mail address: heiner.schumann@sintef.no (H. Schümann).

https://doi.org/10.1016/j.geoen.2023.211599
Received 17 April 2022; Received in revised form 14 February 2023; Accepted 19 February 2023
Available online 22 February 2023

other hand, low shear rates at moderate flow velocities will rather promote droplet coalescence and, together with the density difference between the phases, lead to separation in horizontal flow (Walsh, 2015). In this context, we distinguish between the following scenarios downstream the entrance of an oil-water mixture in a well or flowline: a) increasing oil-water separation, b) stable dispersed flow, or c) increasing oil-water dispersion. Several mixed flow developments are possible. Due to the rather high concentration of stabilizing components in many crude oils, we expect these transitions to happen rather slow leading to transition distances of considerable length in many cases.

The final pressure drop in wells and flowlines, which is strongly dependent on the occurrence of dispersions, is crucial for the possible production rates and total oil recovery rate. Therefore, the dispersion state should be known when choosing preferential pipe geometry, artificial lifting or boosting equipment and even eventual pressure support measures for the reservoir. In addition to the flow resistance, the performance of boosting technologies such as pumps will be influenced by dispersions as documented by Pavlov and Sannæs (2013). Dispersed flow can, in several situations, also be preferential. As an example, high viscosity oil is preferably transported dispersed in water where the pressure drop is significantly lower. On the other hand, free water in pipes may lead to corrosion and, thus, oil continuous flow is preferred from that point of view.

Models for dispersed flow in commercial flow simulators need significant improvements to be reliable design tools. Beside the flow resistance itself, occurrence of dispersed flow, stability of dispersions downstream of pumps and valves, and influence of the fluids' physical properties and chemistry on the aforementioned factors are important characteristics that cannot be predicted with available models.

Detailed experimental data for oil-water pipe flow mainly reports experiments with unstable, fast separating model oil systems (Amundsen, 2011; Elseth, 2001; Angeli, 1996; Schümann, 2016; Trallero, 1995). However, the importance of the fluid system, chemistry and resulting differences between experiments with model oils and real crude oils have been known for a long time, as demonstrated by Valle (2000). Systematic studies, linking the continuous real time droplet size distribution (DSD) and their contribution to the flow development and pressure drop are lacking in particular for fluid systems with droplet stabilizing components. Previous experimental and theoretical studies on evolving oil-water dispersed flow were mainly conducted with the background of describing the development in gravity separators (Hartland and Jeelani, 1988) (Henschke et al., 2002) (Noïk et al., 2013). Even if the same mechanisms are relevant, the geometry of and flow in such a system are considerably different from pipe transport. Dedicated studies investigating flow evolution in pipes with initially dispersed flow were previously conducted by Schümann et al. (2016) and Voulgaropoulos (2017). With a development length of $L/D = 800$ the test section used by Schümann et al. was of considerable length when compared to other oil-water flow studies in the literature. Non-stabilized mineral oil with a medium viscosity was used and a distinct settling behaviour with formation of a dense packed droplet layer observed. A separation model similar to those for gravity settlers was used for predictions. The model was dependent on several parameter tuning. While good results were achieved for low velocities of 0.2 m/s, the model struggled for more dynamic flow at 0.5 m/s. An even longer test section and more realistic fluid systems were recommended for future studies. Voulgaropoulos used a test section with $L/D = 400$ and non-stabilized low viscosity model oil. A similar model approach was tested for the flow of unstable dispersions. Recommended improvements were consideration of the droplet size distribution and droplet interactions such as hindrance. A comprehensive state-of-the-art review of previous experimental studies on evolving flow in unstable systems is also presented in the work by Voulgaropoulos (2017). Still, the summarized data was mentioned to be of rather limited usefulness due to short development length, very limited dispersed phase fractions and insufficient quality of measurements.

The choice of the fluid system and abstinence of dispersion stabilizing agents, providing a fluid behaviour closer to real crude oil systems, is another main shortcoming of existing studies. A typical mixture of two immiscible fluids is thermodynamically unstable as the tendency to reduce interfacial energy enables phase transition or destabilization (ISO/TR 13097 Guidelines for the, 2013). If surface-active compounds or surfactants are present in the system, it's kinetic stability will increase. In flowing two-phase systems stability is affected by both operating conditions and surfactant mass transfer between the phases. This gives a combined effect on dispersion formation and destabilization dynamics. Thus, droplet coalescence, break-up, and their redistribution directly contribute to the resulting flow pattern and flow development.

As crude oils are recovered, oil/water dispersions stabilized by a variety of natural and added surface-active compounds are formed. During transport, single surfactants, or their mixtures, are added to influence formation of a specific dispersion type, water-in-oil (w/o) or oil-in-water (o/w), and obtain the desired stability and flow behaviour. Many production chemicals, for instance corrosion inhibitors, are surface active and can also be seen as surfactants.

Surfactant mass transfer between phases in a two-phase dispersed flow is a dynamic process contributing to the droplet coalescence. As droplets grow in size, the available surface area per unit volume will decrease and surfactants move to the bulk phase. According to an adsorption isotherm, the interfacial surfactant concentration will simultaneously increase causing a significant delay in a drainage of interfacial films between neighbouring droplets, or droplets and their corresponding bulk interfaces (Tadros, 2013). The density difference between the phases, in some cases, is also expected to significantly contribute to the transition between the internal flow structures directly affecting coalescence rates. In oil/water systems, the density difference between the phases is relatively low. Therefore, in addition to the operating conditions, interfacial tension (IFT) and wall-wetting properties of the phases may have a considerable effect on flow development (Brauner, 2002). The interfacial tension results from a force imbalance at the interface between two immiscible fluids, here oil and water. It describes the resistance that needs to be overcome to break this surface in terms of separating the molecules. For a reduced IFT, we will therefore expect smaller droplets to be formed during emulsification. This in turn will influence the resulting flow pattern and dynamic separation behaviour in pipe flow. Khakpay et al. (2009) demonstrated the decrease in IFT and resulting droplet size by addition of surfactant to a mixer-settler setup. Also Omer and Pal (2013) observed droplet size reduction by addition of oil soluble surfactant in pipe flow experiments. Furthermore, a changed rheology was found in terms of increased friction factor and delayed laminar-turbulent transition when surfactant was added. These findings were supported by experiments by Plasencia (2013) adding the oil soluble surfactant Span80 to the fluid system. No study, however, is known to the authors investigating the flow evolution of surfactant stabilized dispersions in pipes.

In the present work we report a unique set of experimental data for transient dispersed flow downstream of a valve. A surfactant was used to partly stabilize the formed dispersions by slowing down coalescence between droplets leading to longer in-flow separation time/distance. At the same time the interfacial tension was reduced by the addition of the surfactant.

The overall objective of the study was to improve our understanding of spatially evolving two-phase oil-water pipe flows downstream of a flow disturbance in the presence of interface stabilizing surfactants. Further, it was the objective to create a detailed data set to be used as basis for future model development work with respect to dynamic flow development. The considerable test section length and the use of surfactant as additive to mimic more realistic crude oil behaviour address shortcomings of previous work. In addition, detailed spatial phase distribution and droplet size measurements can be pointed out as a novelty of the work.

The paper is organized as follows: Section 2 describes the details

regarding the experimental setup, fluids used, test conditions and procedure, and the instrumentation. The experimental results are presented in section 3. First, bench scale experiments screening the stabilization effect of the surfactant used, section 3.1, and a set of flow loop experiments with pure fluids to be used as reference data, section 3.2, are presented. The observed flow development is described in section 3.3 focusing on measured changes in the phase distribution and pressure drop along the test section. Coalescence and sedimentation considerations based on in-situ droplet measurements are described in section 3.4. The influence of different operating parameters on the observed flow development is demonstrated in section 3.5. The conclusion of the study is given in section 4, followed by recommendations for future work, section 5, and the acknowledgements, section 6. References are given in section 7.

2. Experimental procedure

2.1. Setup

Experiments were performed using the so-called Medium Scale Flow Loop in SINTEF's Multiphase Flow Laboratory at Tiller, Norway. A stainless-steel pipe with an inner diameter of $ID = 109.1$ mm was used as test section. The total length of the test section was 220 m and included three 180° bends with a bend radius of 2.25 m, see Fig. 1. The bend effect on the downstream flow was tested and evaluated to be insignificant for the tested fluid system and operating conditions. The main instrumentation of the test section included four optical sections with video recording, three traversing gammas densitometers, nine pressure transducers and three droplet sampling points adjustable in height. The locations of the instrumentation are summarized in Table 1. The test section was inclined by 0.11° so that the second loop could be placed on top of the first one allowing the gamma densitometers to traverse both pipes.

The facility was designed as a closed flow loop where test fluids were returned into a large separator for re-conditioning after passing the test section. From there the clean fluids were extracted and again pumped to the test section inlet. This happened in continuous operation. Flow loops are common to use in such experiments, in order to reduce the required total volume of test fluids, which otherwise would become too much in once through experiments. At the test section inlet, a Y-type junction was used. The junction was fed by separate oil and water lines from the 11 m^3 separator. The separator was used to separate the recirculated fluids. Each feed line was equipped with a centrifugal pump, a Coriolis meter and a control valve used for regulating the flowrates. From the test section outlet, the fluids returned directly to the separator. Additional instrumentation consisted of an absolute pressure transducer in the separator, temperature sensors for oil and water and ports in the feed lines for sample extraction.

Table 1
Locations of instrumentation.

Instrumentation/device	Position from inlet choke valve
ΔP inlet butterfly valve	0 m
Optical sections	1 m, 107 m, 114 m, 219 m
Traversing gamma measurements	2 m, 47 m, 105 m, 160 m, 218 m
Pressure transducers	4 m, 48 m, 60 m, 104 m, 116 m, 161 m, 173 m, 218 m
Droplet sampling probes	1 m, 106 m, 219 m

2.2. Fluid system and test conditions

The fluid system consisted of 6 m^3 of the light mineral oil Exxsol D60 (density; $\rho_o = 789$ kg/m^3, dynamic viscosity: $\mu_o = 1.4$ mPa s) and 4 m^3 tap water (density; $\rho_w = 998$ kg/m^3, dynamic viscosity: $\mu_w = 1.0$ mPa s). Air was present in the separator but was not circulated. All experiments were conducted at room temperature (20 °C) with minor variations and at atmospheric pressure. The non-ionic oil soluble surfactant SPAN 83 (sorbitansesquioleate; HLB 3.7) suitable for obtaining stable w/o dispersions was added to the oil phase at approximately 100 ppm concentration. Span 83 has the molecular formula $C_{66}H_{126}O_{16}$ and is a well-documented product widely used in the cosmetic industry (National Library of Medicine). A 1000 ppm of water-soluble IKM CC-80 biocide (quaternary ammonium salt purchased from Mitco, Norway) was added to the water phase to prevent organic growth during the campaign. Bottle shaking tests confirmed no influence of the biocide on the stability of dispersions formed. The stabilization of w/o dispersions by addition of Span 83 was remarkable and will be explained in more detail in section 3.2. The ppm concentrations in this work are based on weight/weight (w/w) concentrations. Test conditions and fluid properties are summarized in Table 2.

2.3. Test procedure

Each test point was defined by a total mixture velocity, a water cut (WC, common description for the inlet water fraction of the total liquid flow) and a pressure drop over the inlet valve. First, the oil rate was adjusted. Second, the water rate was carefully increased until the desired WC was reached. The order was important to avoid initial

Table 2
Summary of test conditions and fluid properties.

Test condition	Value
Fluids temperature	20 °C
System pressure	1 bara (atmospheric pressure)
Oil phase	Exxsol D60 ($\rho_o = 789$ kg/m^3, $\mu_o = 1.4$ mPa s)
Water phase	Tap water ($\rho_w = 998$ kg/m^3, $\mu_w = 1.0$ mPa s)
Additives – water phase	Biocide 1000 ppm IKM CC-80
Additives – oil phase	Surfactant 100 ppm Span 83

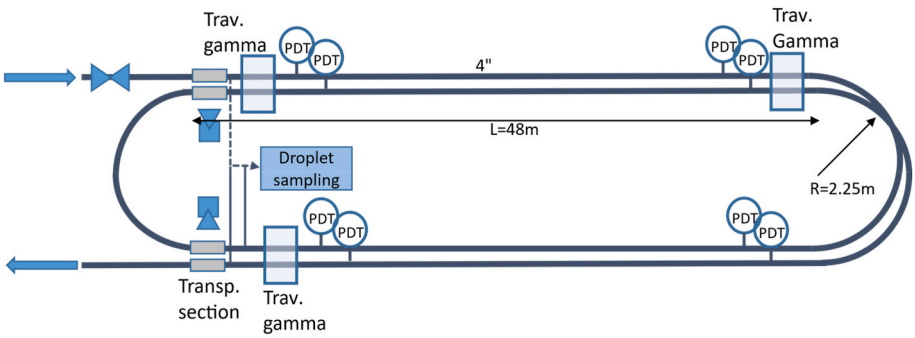

Fig. 1. Sketch of test section with instrumentation.

wetting the inner pipe wall with water. The exception was for separated flows where this could not be avoided. Phase inversion describes the situation where the continuity of dispersed flow suddenly switches as result of exceeding a critical oil/water flow ratio. When switching from water to oil continuous flow hydrophilic steel pipes tend to maintain a thin water film on the pipe wall which will require rather high oil rates or a long time to be washed away. This film can be critical for oil dominated flow. Test points were obtained from low to high WCs. In case when inlet mixing was used, the initially fully open valve was slowly choked until the desired pressure drop over the valve was reached. The auto-controlled flowrates were kept constant. Consecutive instrumentation showed that the flow with fully open valve was developed after approximately 100 m. Logging of steady state test points was first started once all instrumentation reached constant readings. Time averaged measurements of a logging period of approximately 10 min are presented in this work.

2.4. Instrumentation

2.4.1. Pressure measurements

Pressure taps were mounted in the pipe wall in horizontal orientation. In this way the type of fluid filling the pressure taps will not contribute to a hydrostatic pressure. Differential pressure transducers of type Fuji Electric-FCX series were used for all pressure taps. The reported pressure gradient was calculated as the pressure difference between consecutive cells divided by the distance. The measurement uncertainty was 0.065% of 5 bar range.

2.4.2. Traversing gamma densitometry

A collimated barium source and gamma detector were mounted to a vertically traversable mechanism as shown in Fig. 2. Since the two loops of the test section pipe were placed on top of each other, it was possible to scan two pipe section positions with each traversing gamma instrument. The gamma beams are traversed to measure the cross-sectional phase distribution. By slowly traversing the setup across the pipe and knowing the attenuation for a completely oil and water filled pipe (calibration) the in-situ phase fractions at each height can be determined. The produced profiles indicate phase distributions inside the pipe. Note that the horizontal phase distribution across the pipe was not measured.

2.4.3. Droplet sampling

A 6 mm *ID* probe, as sketched in Fig. 3, was used for quasi iso-kinetic sampling. Quasi iso-kinetic because the nominal flow velocity was used to determine the sampling rate, however, the exact in-situ velocity profile was not considered. The probe was connected to a CANTY InFlow™ particle sizer, which is a flow-through device producing high resolution pictures. Pictures were analysed in post-processing to obtain at least 500 droplet counts per sample location. The influence on droplet sizes of the short sampling tube between pipe and CANTY device was evaluated by varying the sampling line length for otherwise identical conditions in test measurements. No change was found. The probe position could be adjusted in vertical direction. Samples were taken 3 cm from top, 3 cm from the bottom and in the centre of the pipe. Based on experience, we estimate the uncertainty of the reported characteristic droplet sizes to be within 10%.

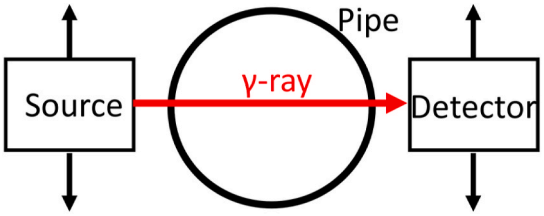

Fig. 2. Sketch of the traversing gamma instrument and beam path.

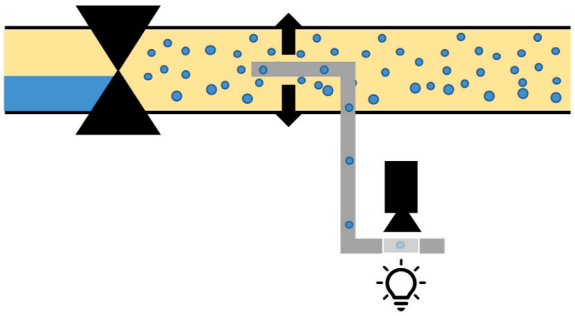

Fig. 3. Sketch of the setup for droplet sampling.

2.4.4. Interfacial tension measurements

Interfacial tension (IFT) of fluid samples was used to estimate the real SPAN 83 concentration in the circulated oil. A TRACKER tensiometer by TECLIS-I.T.C. was used for the measurements of fluid samples. The IFT of oil droplets rising from a siring in water was measured. A calibration curve of SPAN 83 concentration as a function of IFT was created from samples of oil and water taken from the separator before SPAN 83 was introduced to the system. Known concentrations of SPAN 83 were added to the oil and the IFT measured. Thus, the calibration curve used the same fluids as used during the experiments including possible impurities from the flow loop and the IKM CC-80 biocide initially added to the water phase. A polynomial function found from a curve fit was thereafter used to estimate the SPAN 83 concentration in the fluid samples. The resulting surfactant concentration curve is shown in Fig. 4 as blue curve. Calibration measurements are shown as blue circles. The curve flattens out towards a value of 200 ppm which is approximately the critical micelle concentration (CMC) of the surfactant. The fluid samples were taken right after each experiment was finished.

3. Results and discussion

3.1. Fluid stabilization

The right choice of surfactant and oil phase for formulating water-in-oil (w/o) dispersions was an important aspect of this study. It can be chosen by evaluating the similarities in the molecular structure of the surfactant and the dispersion medium. A hydrophobic-lipophilic balance

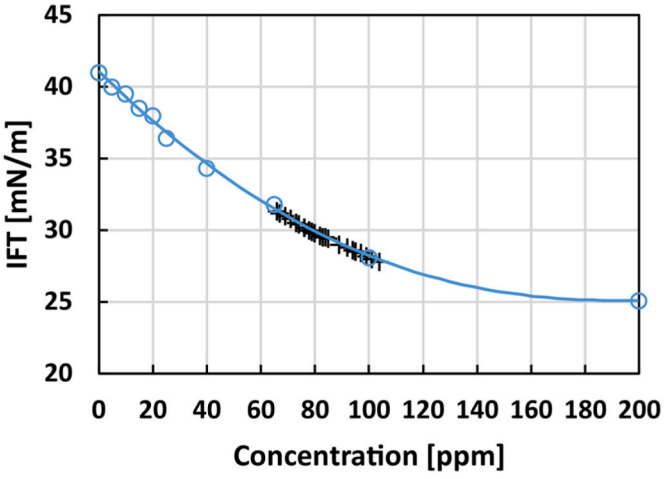

Fig. 4. Interfacial tension as function of surfactant concentration. The blue curve is based on calibration measurements for known concentrations (blue circles). Black crosses represent IFT measurements of the samples taken during the campaign. Test conditions: T = 20 °C, P = 1bara (atmospheric pressure).

(HLB) (Griffin, 1950), or the Bancroft's rule (Bancroft, 1913), states that the phase in which the surfactant is more soluble in will become the continuous phase. The type of resultant dispersion and droplet size distribution (DSD) are also affected by the preparation method, the phase volume fractions, and the viscosities of the involved phases (Davies, 1957). Based on the HLB concept, surfactants with a low HLB value of three to six will normally form w/o dispersions. Span 83 is a biobased nonionic surfactant with HLB of 3.7. It was chosen due to its' good solubility in mineral oils, such as Exxsol D60. Exxsol D60 is a paraffinic light oil with high chemical and oxidative stability. It is commonly used in research purposes as a model oil for studying flow dynamics, separation, and phase changes under fluid transport (Ibarra and Nossen, 2019; Ohrem et al., 2019; Utvik et al., 2001; Elseth, 2001; Amundsen, 2011). Both Exxsol D60 and water exhibit similar and low viscosities. Therefore, the effects of flow development and droplet size evolution of two immiscible low viscosity fluids, was studied in our case.

Span 83 was added to the oil phase to achieve higher stability of w/o dispersions and to prevent immediate separation in the test section downstream of the valve. For the reported experiments, a fixed amount of surfactant was present in the system. The measured average Span 83 concentration in the oil was 85 ppm. This was found by comparing interfacial tension (IFT) measurements from samples regularly taken during the campaign with a calibration curve indicating the change in IFT with surfactant concentration. Measurements from fluid samples are indicated by crosses in Fig. 4. Two reasons for the variation of the sample concentration can be mentioned. First, uncertainty of IFT measurements, and second and more important, real concentration variations over time due to surfactant migration and accumulation in the dispersion layer in the separator. The latter is a known problem in recirculation flow loops. In order to reduce this effect, the flow loop was stopped for a certain time after each test point to achieve better separation of dispersions in the separator. By this, variations were kept within the shown range, but not avoided completely.

The stability of dispersions with different concentrations of Span 83 was tested by shaking tests. Results are presented in Fig. 5 in form of separation curves. 50 ml samples of known WC were vigorously shaken for 30 s and left for separation. The height of the initially dispersed phase that had separated out was measured as function of time. Even if not fully representative for a flowing system, clear tendencies were found. For oil continuous dispersions (e.g. 25% WC), Fig. 5 A, the separation time gradually increased up to a concentration of 50 ppm Span 83. For higher concentrations, a final stable dispersion layer was achieved and mainly the final amount of the separated dispersion varied. For water continuous systems (e.g. 75% WC), Fig. 5 B, all samples separated immediately and independently of the Span 83 concentration. This confirmed, as described earlier, that the chosen surfactant only had a stabilizing effect in the case of w/o dispersions.

3.2 Reference experiments.

The test matrix in Fig. 6 shows the combinations of WC and U_{mix} tested in this work. The main focus was on the low WCs in the oil dominated region. Reference experiments were performed without inlet choking. It is expected that the flow is fully developed at the end of the pipe for these experiments. Inlet choking was only tested for points shown as red filled dots. For these experiments, two different WCs, 20% and 30%, were used to investigate the effect of the droplet phase fraction. Two different U_{mix}, 1 m/s and 1.5 m/s, were used to investigate the influence of the flow velocity on the DSD and subsequent flow development. Comparing these results with the reference experiments will indicate how far the flow is from the final developed state.

For the reference experiments, results from the last measurement position are shown in Figs. 7 and 8. Without inlet choking, the flow reaches developed state rather fast. For most of the test points this was the case after approximately 100 m distance.

Fig. 7 presents water fraction profiles for the reference experiments, showing the local water fractions at different heights in the pipe. For 1 m/s, the flow is separated with a sharp interface for all WCs. At 1.5 m/s, the interface becomes more diffuse, likely due to some droplets formed and recorded in the measurements. Two continuous regions, oil on top and water at the bottom of the pipe, can still be identified. At 2 m/s, intensified internal mixing contributes to increased droplet volume fraction as the flow starts to turn into fully dispersed state. The inhomogeneity is still present because of large droplet sizes in the flowing system, where turbulent diffusion does not overcome gravitational forces.

Corresponding pressure drop measurements are shown in Fig. 8. For the separated flow experiments at 1 m/s (blue circles) the measurements lie between the values for single phase oil and water. For the higher velocities (1.5 m/s red squares, 2 m/s yellow triangles) with presence of dispersion, a slight drag reduction behaviour can be observed where the

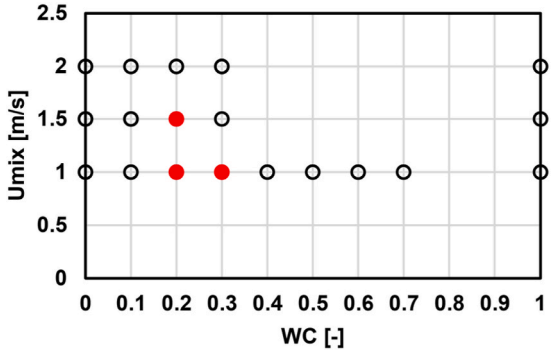

Fig. 6. Experimental matrix. Experiments with inlet choking were performed for the filled red dots.

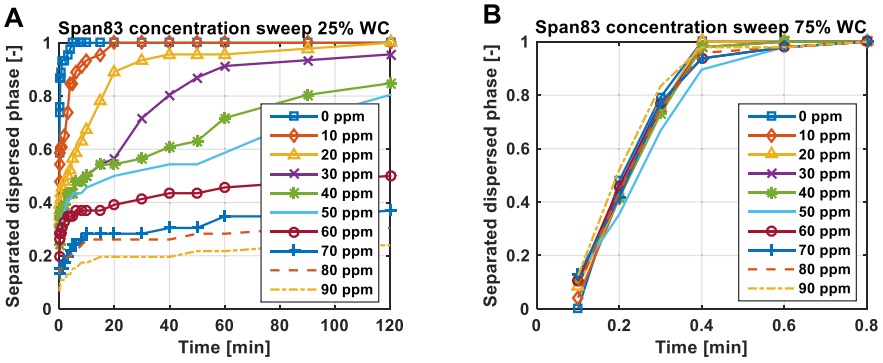

Fig. 5. Separation curves from shaking tests for different Span 83 concentrations: 25% WC (A), 75% WC (B). Test conditions: T = 20 °C, P = 1bara (atmospheric pressure).

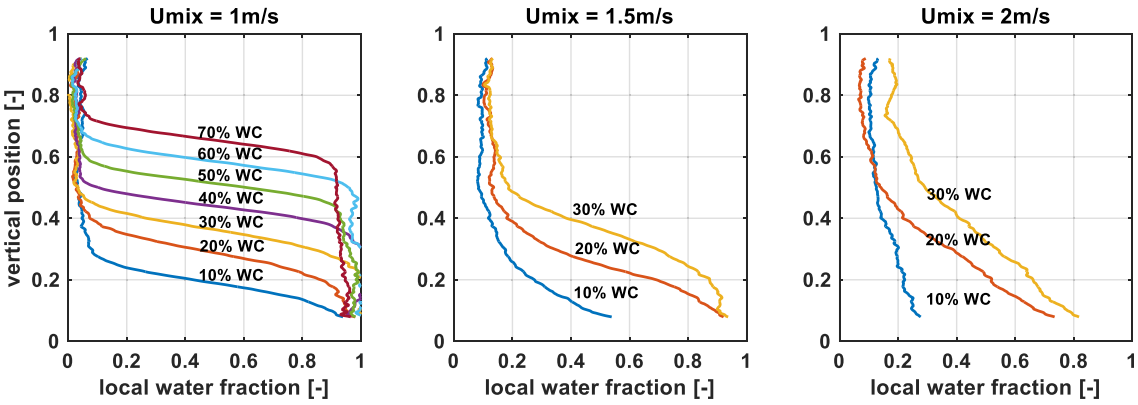

Fig. 7. Water fraction profiles for the experiments without inlet choking. Test conditions: T = 20 °C, P = 1bara (atmospheric pressure).

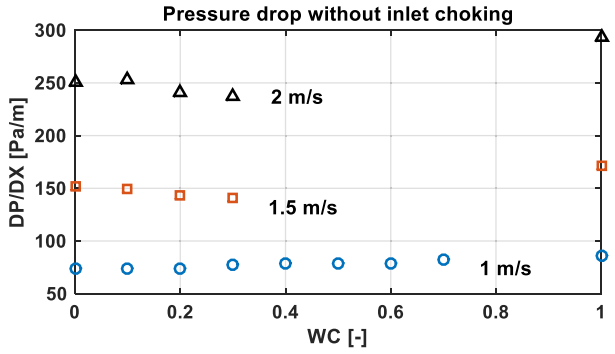

Fig. 8. Pressure drop in developed flow without inlet choking. Blue circles for 1 m/s, red squares for 1.5 m/s and yellow triangles for 2 m/s. Test conditions: T = 20 °C, P = 1bara (atmospheric pressure).

pressure drop falls below the value for a single phase oil. This behaviour agrees with observations from other authors (Angeli and Hewitt, 1998; Kumara et al., 2008; Soleimani, 1999). Pal (1993) mentioned the dynamic break-up and coalescence behaviour of droplets to be responsible for drag reduction while the effect disappears for stable dispersions. Based on that one might argue that our fluid system is partly stabilized with coalescence still taking place at a reduced rate due to surfactant interference.

3.2. Flow development

Local water fraction profiles for WC = 20% and U_{mix} = 1.0 m/s are presented in Fig. 9 for five locations along the pipe. Each plot shows experiments with a different pressure drop over the inlet mixing valve of 0.2 bar (Fig. 9 A), 0.35 bar (Fig. 9 B), 0.5 bar (Fig. 9 C) and 1 bar (Fig. 9 D). A clear development of the flow can be observed. Initially the phase fractions are rather homogeneously distributed over the cross section. Then the flow separates rather suddenly between two measurement positions, except in the case of DP_{valve} = 1.0 bar. This is indicated by a high local water concentration in the bottom layer of the pipe and

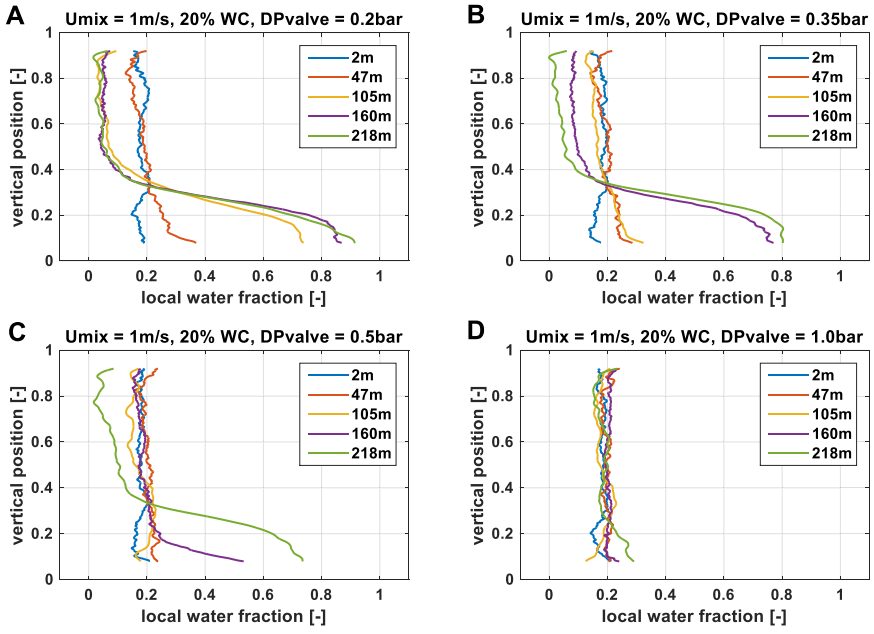

Fig. 9. Water fraction profiles downstream of the choke valve for Umix = 1 m/s and 20% WC. Four different pressure drops over the choke valve were tested: 0.2 bar (A), 0.35 bar (B), 0.5 bar (C), 1.0 bar (D). Test conditions: T = 20 °C, P = 1bara (atmospheric pressure).

simultaneously a reduced water amount in the upper pipe region. The separation distance after the valve strongly depends on the pressure drop over the valve, and arguably inversely related to the initial droplet sizes created inside the valve. For the highest tested pressure drop over the valve, no separation was observed along the test section. Only the last measurement position indicates a slightly higher water concentration in the bottom. It should be mentioned that real choke valves in production equipment can reach much higher pressure drops (several bars), contributing significantly to the downstream multiphase flow behaviour over long distances.

An average dispersion factor (ADF) representative for the whole pipe cross-section was derived. First, a local dispersion factor was calculated to quantify the droplet dispersibility in different layers as shown in Fig. 10. Here, the local water fraction measurements were weighted with the local (height dependent) width of the pipe and integrated over the height. The local average dispersion factors (in %) were then calculated as follows:

$$ADF_{top} = 100\% * \left[1 - \frac{(WC - LWF)}{WC}\right], \quad (1)$$

$$ADF_{middle} = 100\% * \left[1 - \frac{(LWF - WC)}{WF_{ref}}\right], \quad (2)$$

$$ADF_{bottom} = 100\% * \left[1 - \frac{(LWF - WC)}{(1 - WC)}\right], \quad (3)$$

where LWF is the local water fraction and WF_{ref} is a reference water fraction for the middle layer at separated conditions covering the interface region. For example, the local ADF will be 100% with the LWF equal to the WC of the test point; and 0% when the LWF is zero in the top layer or 1 in the bottom layer. The total ADF then represents the complete cross section.

A comparison of the total ADF together with the measured pressure drop in the pipe for the different choking values is shown in the plots in Fig. 11.

The axial development of the ADF and pressure drop correlates in all four experiments. However, a delay is observed for higher choking values. For the highest choking of $DP_{valve} = 1$ bar the measurements along the pipe are relatively constant and no clear separation behaviour or change in the pressure drop was observed at all. The multiphase flow development downstream the choke valve can be described as a balance between turbulent dispersive forces and gravitational forces, the latter leading to droplet sedimentation. In addition, droplets will coalesce. The droplet break-up rate is expected to be insignificant because the reference flow pattern (which can be seen as the fully developed flow) is separated and initial droplets created in the inlet valve are already small. Therefore, at the test section entrance, just after the valve, water droplets might be too small to settle immediately and will be kept dispersed by the turbulent flow. Presumably this is the case for $DP_{valve} = 1$ bar throughout the test section. For the other cases, with proceeding coalescence, a critical droplet size will be reached and gravitational force

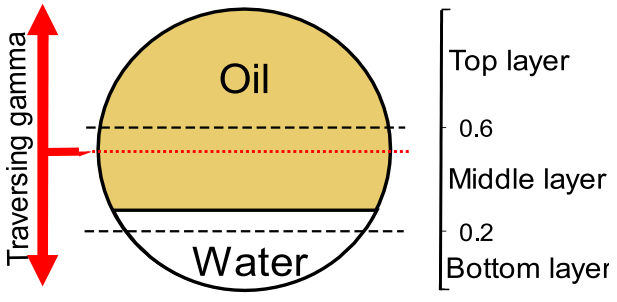

Fig. 10. Layer definition for calculation of the Average Dispersion Factor, ADF. The example shows a separated system.

dominate such that droplets settle. The separation rate arguably passes through a maximum (as can be observed as a steep decline of the ADF curve in Fig. 11) before further coalescence is hindered. Presumably, the smallest droplets will stay dispersed at low concentration and reduced coalescence rate. For a small concentration, the collision rate of droplets is lower and local surfactant coverage higher. The dense packed droplet layer that might form at the oil-water interface will also hinder further coalescence with the water interface. Note that the water fractions in the bottom part of the pipe in Fig. 9 never reach one. This could indicate the presence of a very tight dispersion. The pressure drop seems to reach a local minimum for a certain dispersion factor (around 40%). Here, the pressure drop is slightly higher than for the reference separated flow experiments shown in Fig. 8. Further separation leads to increasing pressure drop. The reason is not clear and needs further investigation. One possibility is that the before mentioned build-up of a dense water-in-oil dispersion over time at the interface or in the bottom of the pipe causes this pressure drop increase. The effective viscosity in such a layer can be very high. This in turn will lead to high wall shear stress. If this is the case, one would expect that the pressure drop reduces again as the dense-packed layer disappears. Unfortunately, even our 220 m long test section was too short to obtain reliable observations thereof.

3.3. Coalescence and sedimentation

Droplet sizes were measured and correlated to the local separation state. Fig. 12 shows an example image for 1 m/s and 20% WC with 0.2 bar pressure drop over the inlet choke valve. A large variation of droplet sizes from a few μm to several hundred μm can be observed.

The images were processed to obtain local droplet measurements at different positions in the pipe (vertical direction) and along the pipe (downstream of the valve). The Sauter mean diameters, D_{32}, are compared in this study. Fig. 13 shows the D_{32} at the different measurement locations for the same experiments as discussed before. A typical behaviour can be observed. At the inlet, the D_{32} across the pipe is more uniform considering the uncertainty in measured droplet sizes. Also, the initial droplet sizes become smaller with increasing pressure drop over the choke valve. Further downstream the pipe the largest droplets will settle to the bottom of the pipe while the smallest droplets remain dispersed across the pipe. D_{32} values below 100 μm are typically observed in the upper part at the end of the test section, indicating a critical droplet size required for sedimentation. For the experiment with 1 bar pressure drop over the choke valve, measurements are very similar for all positions. Initial droplets are small (approximately 80 μm) and the coalescence rate not high enough to produce droplets of sufficient size needed for sedimentation within the restricted test section length.

Evolution of droplet sizes (cross sectional averages) for different positions along the pipe and the four different choking values are presented in Fig. 14. Droplets grow slowly in the beginning as small droplets coalesce into larger ones. Downstream the pipe the growth rate increases due to the coalescence of larger droplets. In addition, a higher droplet concentration in the lower pipe region due to sedimentation will increase the collision frequency in this region and lead to higher coalescence rates. Therefore, droplet growth rates are higher for the experiments with lower pressure drop over the choke valve where initially larger droplets sediment faster. Vice versa, higher choking will generate smaller droplets. These droplets will initially sediment slower or not at all if small enough. Thus, separation and coalescence rates will be smaller.

3.4. Influence of operating conditions

Additional experiments with inlet choking were performed for comparison with the previously presented results at 1 m/s and 20% WC. Experiments at 1 m/s and 30% WC were used to investigate the effect of WC. Experiments at 1.5 m/s and 20% WC were used to investigate the effect of flow velocity. Fig. 15 shows water fraction profiles for 1 m/s

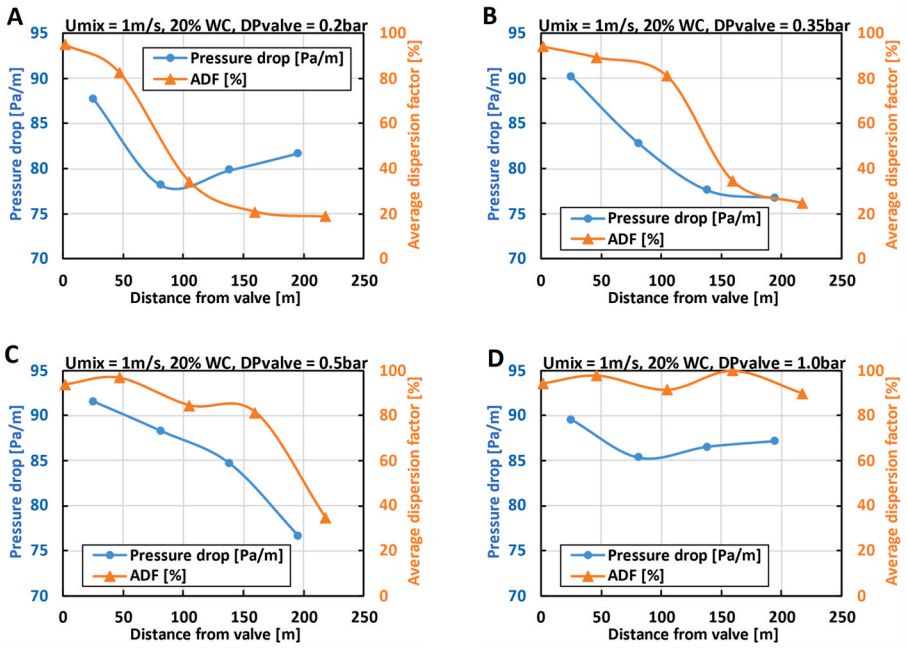

Fig. 11. Pressure drop and ADF for Umix = 1 m/s and 20% WC. Four different pressure drops over the choke valve were tested: 0.2 bar (A), 0.35 bar (B), 0.5 bar (C), 1.0 bar (D). Test conditions: T = 20 °C, P = 1bara (atmospheric pressure).

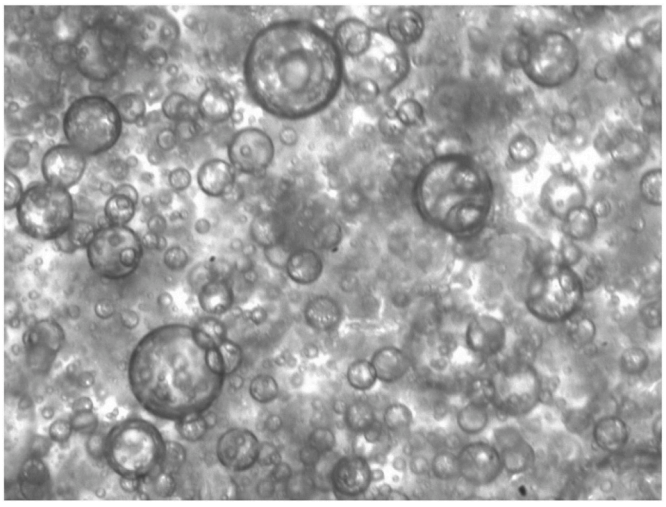

Fig. 12. Picture from the CANTY droplet monitoring device. The dimension is 2400 μm × 1800 μm.

and 30% WC. Comparison with Fig. 9 shows that the separation behaviour is very similar and no significant difference in the separation length and profiles was found. Of course, the interface height at separated conditions will change due to the higher amount of water. For very low WCs, meaning low dispersed phase fractions, a lower coalescence rate due to a lower droplet collision frequency can be expected. Such experiments, however, were not performed. This can be seen as a drawback of the study and should be considered in future work.

The influence of the U_{mix} on the flow development was investigated by comparing the ADF and pressure drop along the pipe. The results for 1.5 m/s are shown in Fig. 16 for choking of 0.2 and 0.35 bar. When compared with 1 m/s (Fig. 11), a similar general behaviour is observed. However, the onset of separation as well as the location of the dip in the pressure drop curve are shifted towards longer distances. More precisely separation occurs at approximately 50% longer distance from the valve. One may thus argue that the flow development distance studied can simply be scaled by U_{mix}. Based on this, it can be argued that the governing mechanism in the flow is coalescence and not turbulence-controlled break-up of droplets. In the latter case, higher U_{mix} would lead to a longer separation time scale due to delayed droplet growth and separation. A coalescence dominated behaviour was also expected for the surfactant stabilized system.

4. Conclusion

Flow development of a surfactant stabilized two-phase oil/water system in a 220 m long flow loop was studied. A valve was used to mix the phases at the test section inlet. Traversing gamma densitometry was used to measure the cross-sectional phase fraction profiles and by this the dispersed state of the flow. An average (across the pipe) local (along the pipe) dispersion factor was defined and used as measure for the in-situ separation. The observed separation downstream of the valve had a characteristic behaviour with a sudden onset. This onset showed a strong dependency on the initial mixing intensity in the valve and thus initial droplet size. Subsequent separation happened rather fast but incomplete. Coalescence hindering in a dense droplet layer forming at the bottom of the pipe was suspected to delay the final complete separation and formation of a free water layer.

Comparison of in-situ droplet size measurements showed that the droplet growth rate increases with progressing separation. This might be explained by increasing droplet collision frequency in the lower part of the pipe where the droplet concentration increases with proceeding separation. Turbulent flow is required for the mechanism of increased droplet collision. At very high droplet concentration the local flow will become laminar and the beforementioned effect of coalescence hindering of film drainage will be governing. Therefore, the two effects don't stand in contrast to each other.

The pressure drop in the pipe is related to the flow pattern and changed along with the in-situ separation. The initial pressure drop for dispersed flow was approximately 20% higher than for separated flow at the same conditions.

The effects of flow rate and water cut on the flow development were also investigated with a limited number of experiments. As expected, flow development length correlated with U_{mix} but the separation time

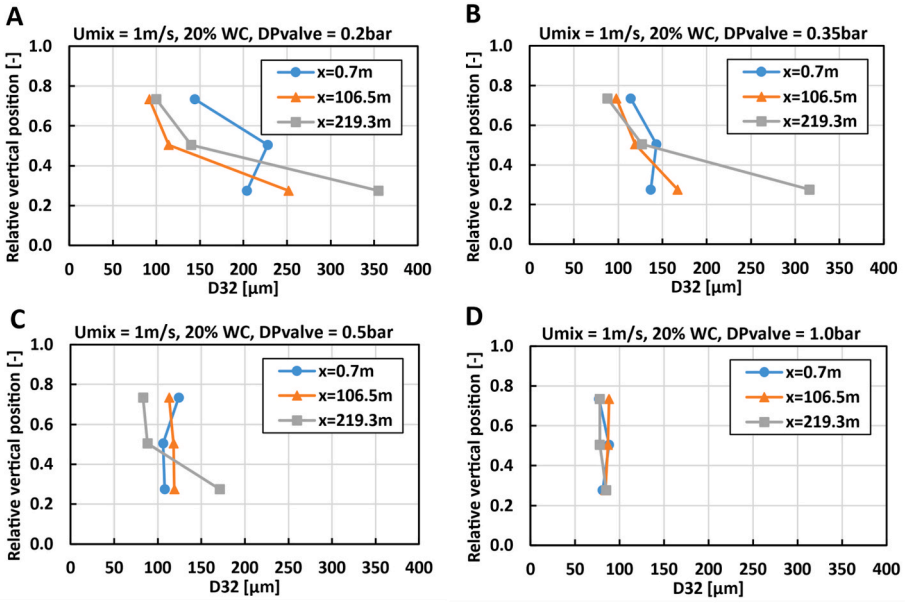

Fig. 13. Sauter mean diameter, D32, for different measurement positions in the test section for Umix = 1 m/s and 20% WC. Four different pressure drops over the choke valve were tested: 0.2 bar (A), 0.35 bar (B), 0.5 bar (C), 1.0 bar (D). Test conditions: T = 20 °C, P = 1bara (atmospheric pressure).

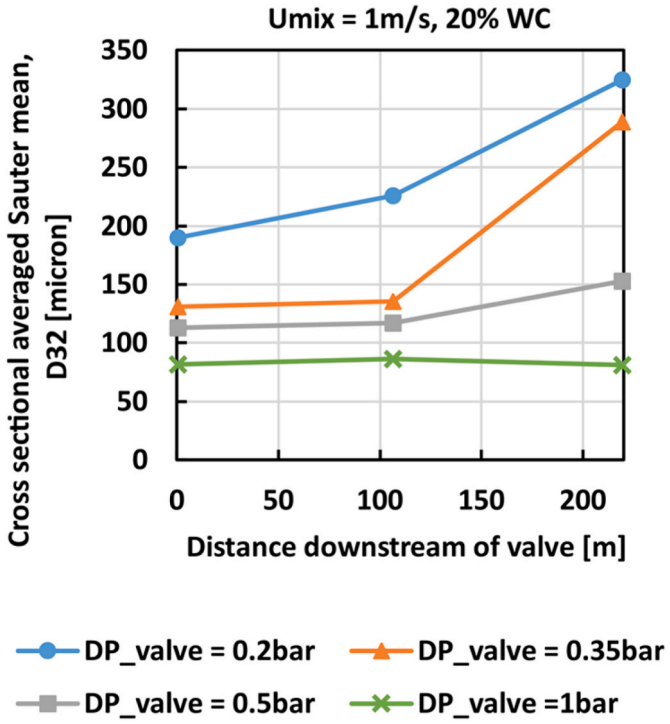

Fig. 14. Droplet growth downstream of the choke valve for Umix = 1 m/s and 20% WC. Test conditions: T = 20 °C, P = 1bara (atmospheric pressure).

was unchanged. No effect was found when WCs of 20% and 30% were compared. Our results suggest that under otherwise constant conditions, the onset of separation in surfactant stabilized oil-water pipe flow may to the first order be scaled with U_{mix}.

When compared with static bench tests, the flow separation in a flowing system happened considerably faster. This indicated for separation favorable conditions in the dynamic system studied. Still, for comparable surfactant concentrations, in both systems the separation was incomplete. However, the test section length was restricted and a final state not reached.

5. Recommendations for future work

A drawback of the study was the incomplete monitoring of the flow development to fully separated flow. It is therefore recommended to increase the test section length. This would further enable to test more realistic operating conditions such has higher U_{mix} and higher choking at the inlet.

The study focused on a very restricted set of parameters. Similar experiments with a wider parameter range such as different oil viscosities, different types of surfactant and surfactant concentrations or even real crude oils with different stabilities would be needed to get a better basis for understanding and finally model development. Finally, also the interaction with a gas phase in three phase flow is uncertain and should be considered for future work.

Regarding the instrumentation it was not fully clear what happened in the different regions of the pipe and how the phase distribution can be exactly related to the pressure drop. Improved instrumentation for more detailed phase distribution monitoring, wall wetting measurements and measurements of velocity profiles is recommended.

Finally, the gained knowledge should be translated into dynamic flow models which are able to predict flow development based on a given dispersion state of the flow at a specific location, which can be provided as input or predicted by sub-models for valves, pumps or similar.

Credit author statement

Heiner Schümann: Conceptualization, Methodology, Validation, Formal analysis, Investigation, Resources, Data curation, Writing – original draft, Visualization, Supervision, Project administration, Funding acquisition, **Galina Simonsen**: Conceptualization, Methodology, Investigation, Writing – original draft, **Christian Brekken**: Methodology, Formal analysis, Writing – review & editing.

Declaration of competing interest

The authors declare the following financial interests/personal relationships which may be considered as potential competing interests: Heiner Schumann, Galina Simonsen, Christian Brekken reports financial support was provided by TotalEnergies EP Norge AS.

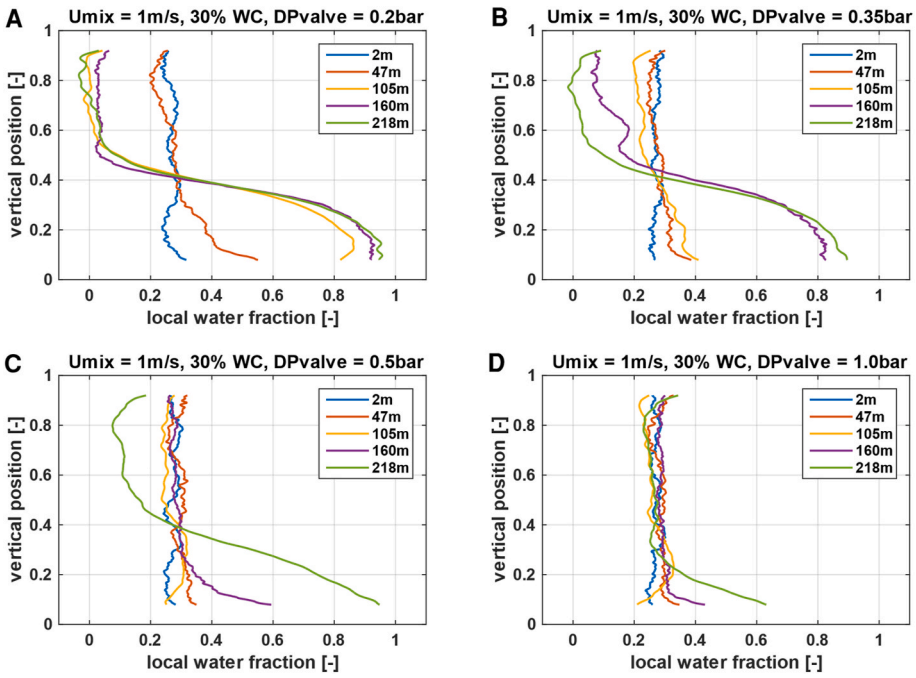

Fig. 15. Water fraction profiles downstream of the choke valve for Umix = 1 m/s and 30% WC. Four different pressure drops over the choke valve were tested: 0.2 bar (A), 0.35 bar (B), 0.5 bar (C), 1.0 bar (D). Test conditions: T = 20 °C, P = 1bara (atmospheric pressure).

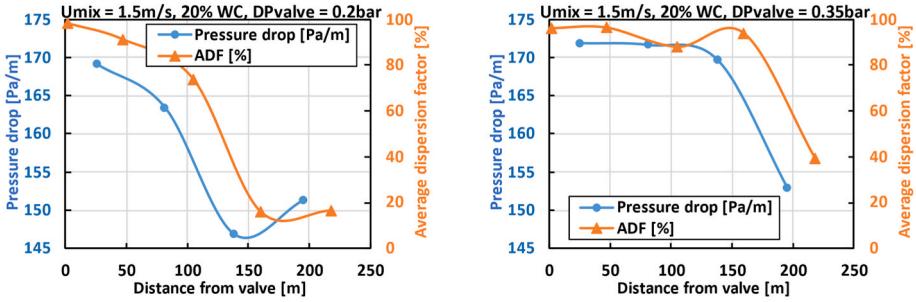

Fig. 16. Pressure drop and ADF for Umix = 1.5 m/s and 20% WC. Two different pressure drops over the choke valve are shown: 0.2 bar (A), 0.35 bar (B). Test conditions: T = 20 °C, P = 1bara (atmospheric pressure).

Data availability

Data will be made available on request.

Acknowledgements

The work is a joint effort of a SINTEF financed project on oil-water dispersions (OWAD) and the knowledge-building project for industry (NFR project number 295035) Nexflow, which would not have been possible without the financial support by TotalEnergies EP Norge AS and the Research Council of Norway.

References

Amundsen, L., 2011. An Experimental Study of Oil-Water Flow in Horizontal and Inclined Pipes, PhD Thesis. Department of Energy and Process Engineering. Norwegian University of Science and Technology, Trondheim.

Angeli, P., 1996. Liquid-liquid Dispersed Flows in Horizontal Pipes, PhD Thesis. Imperial College of Science, Technology and Medicine, London.

Angeli, P., Hewitt, G., 1998. Pressure gradient in horizontal liquid-liquid flows. Int. J. Multiphas. Flow 24, 1183–1203. https://doi.org/10.1016/S0301-9322(98)00006-8.

Bancroft, W.D., 1913. The theory of emulsification. J. Phys. Chem. 17 (6), 501–519, ttps://doi.org/10.1021/j150141a002.

Brauner, N., 2002. Modelling and Control of Two-phase Phenomena: Liquid–Liquid Two-phase Flow Systems. School of Engineering Tel Aviv University, Tel Aviv.

Davies, J.T., 1957. A quantitative kinetic theory of emulsion type, I. Physical chemistry of the emulsifying agent. In: 2nd International Congress of Surface Activity. Butterworths, London, UK.

Elseth, G., 2001. An Experimental Study of Oil/Water Flow in Horizontal Pipes, PhD Thesis. The Norwegian University of Science and Technology.

Griffin, J., 1950. Emulsions, encyclopedia of chemical technology. In: Kirk and Othmer. Interscience, New York.

Hartland, S., Jeelani, S., 1988. Prediction of sedimentation and coalescence profiles in a decaying batch dispersion. Chem. Eng. Sci. 43 (9), 2421–2429. https://doi.org/10.1016/0009-2509(88)85176-5.

Henschke, M., Schlieper, L., Pfennig, A., 2002. Determination of a coalescence parameter from batch-settling experiments. Chem. Eng. J. 85 (2–3), 369–378. https://doi.org/10.1016/S1385-8947(01)00251-0.

Ibarra, R., Nossen, J., 2019. Investigation of oil-water flow in concentric and fully eccentric annuli pipes. Chem. Eng. Sci. X 4, 100042. https://doi.org/10.1016/j.cesx.2019.100042.

ISO/TR 13097 Guidelines for the Characterization of Dispersion Stability, 2013.

Khakpay, A., Abolghasemi, H., Salimi-Khorshidi, A., 2009. The effects of a surfactant on mean drop size in a mixer-settler extractor. Chem. Eng. Process: Process Intensif. 48 (6), 1105–1111. https://doi.org/10.1016/j.cep.2009.02.003.

Kumara, W., Halvorsen, B., Melaaen, M., 2008. Pressure drop, flow pattern and local water fraction measurements of oil-water flow in pipes. Meas. Sci. Technol. 20 https://doi.org/10.1088/0957-0233/20/11/114004.

National Library of Medicine. Span 83 (=Sorbitan sesquioleate). National Center for Biotechnology Information, [Online]. Available: https://pubchem.ncbi.nlm.nih.gov/compound/Span-83-_Sorbitan-Sesquioleate.

Noïk, C., Palermo, T., Dalmazzone, C., 2013. Modeling of liquid/liquid phase separation: application to petroleum emulsions. J. Dispersion Sci. Technol. 34. https://doi.org/10.1080/01932691.2012.735929.

Ohrem, S.J., Slettahjell Skjefstad, H., Stanko, M., Holden, C., 2019. Controller design and control structure analysis for a novel oil–water multi-pipe separator. Processes 7 (4), 190. https://doi.org/10.3390/pr7040190.

Omer, A., Pal, R., 2013. Effects of surfactant and water concentrations on pipeline flow of emulsions. Ind. Eng. Chem. Res. 52 (26). https://doi.org/10.1021/ie3036492.

Pal, R., 1993. Pipeline flow of unstable and surfactant-stabilized emulsions. AIChE J 39 (11), 1754–1764. https://doi.org/10.1002/aic.690391103.

Pal, R., 1996. Effect of droplet size on the rheology of emulsions. AIChE J 42 (11). https://doi.org/10.1002/aic.690421119.

Pal, R., Rhodes, E., 1989. Viscosity/concentration relationships for emulsions. J. Rheol. 33. https://doi.org/10.1122/1.550044.

Pavlov, A., Sannæs, B., 2013. Experimental studies of ESP performance with two-phase fluids with live viscous oils. In: World Heavy Oil Congress. Aberdeen.

Plasencia, J., 2013. Experimental study on two phase oil-water dispersed flow. PhD Thesis, Department of Energy and Process Engineering. Norwegian University of Science and Technology: Trondheim..

Schümann, H., 2016. Experimental Investigation of Transitional Oil-Water Pipe Flow, PhD Thesis. The Norwegian University of Science and Technology, Trondheim.

Schümann, H., Chandra, P., Nydal, O., 2016. Oil-water pipe flow development after a valve. In: 9th International Conference on Multiphase Flow. Florence, Italy.

Soleimani, A., 1999. Phase Distribution and Associated Phenomena in Oil-Water Flows in Horizontal Tubes, PhD Thesis. University of London, London.

Tadros, T., 2013. Encyclopedia of Colloid and Interface Science. Springer-Verlag Berlin Heidelberg.

Trallero, J., 1995. Oil-water Flow Patterns in Horizontal Pipes, PhD Thesis. The University of Tulsa.

Utvik, O.H., Rinde, T., Valle, A., 2001. An experimental comparison between a recombined hydrocarbon-water fluid and a model fluid system in three-phase pipe flow. J. Energy Resour. Technol. 123 (4), 253–259. https://doi.org/10.1115/1.1410365.

Valle, A., 2000. Three Phase Gas-Oil-Water Pipe Flow. PhD Thesis.Department of Chemical Engineering and Chemical Technology. Imparial College of Science, Technology and Medicine, London.

Voulgaropoulos, V., 2017. Dynamics of Spatially Evolving Dispersed Flows. PhD Thesis. University College London, London.

Walsh, J., 2015. The savvy separator series: Part 5. The effect of shear on produced water treatment. Oil & gas Fac 5, 16–23.